HNPS Advances in Nuclear Physics

Hellenic Nuclear Physics Society

HNPS: **Advances in Nuclear Physics**

Proceedings of the 28th Hellenic Conference on Nuclear Physics

Aristotle University of Thessaloniki

May 31st - June 1st 2019

Editors
T. Gaitanos
A. Ioannidou
C. Moustakidis
S. Stoulos

HNPS: Advances in Nuclear Physics · 28th Hellenic Conference

Editors: T. Gaitanos, A. Ioannidou, C. Moustakidis, S. Stoulos

Study of the 165Ho(n,2n)164Ho reaction at near threshold energies

Efstathia Georgali, N. Patronis, A. Anastasiadis, M. Axiotis, Z. Eleme, S. Harissopulos, A. Kalamara, K. Karfopoulos, M. Kokkoris, A. Lagoyannis, M. Peoviti, C. Potiriadis, M. I. Savva, I. Stamatelatos, M. E. Stamati, A. Stamatopoulos, T. Vasilopoulou, R. Vlastou

Study of the ^{165}Ho(n,2n)^{164}Ho$^{g−m}$ reaction at near threshold energies

E. Georgali[1], N. Patronis[1], A. Anastasiadis[2], M. Axiotis[3], Z. Eleme[1], S. Harissopulos[3], A. Kalamara[4], K. Karfopoulos[5], M. Kokkoris[4], A. Lagoyannis[3], M. Peoviti[1], C. Potiriadis[5], M. I. Savva[6], I. Stamatelatos[6], M. E. Stamati[1], A. Stamatopoulos[4], T. Vasilopoulou[6], R. Vlastou[4]

[1] Department of Physics, University of Ioannina, 45110 Ioannina, Greece
[2] Department of Physics and Astronomy, Uppsala University, SE-751 05 Uppsala, Sweden
[3] Tandem Accelerator Laboratory, Institute of Nuclear and Particle Physics, N.C.S.R. "Demokritos", Aghia Paraskevi, 15310 Athens, Greece
[4] Department of Physics, National Technical University of Athens, Zografou Campus, 15780 Athens, Greece
[5] Environmental Radioactivity Monitoring Department, Greek Atomic Energy Commission, Aghia Paraskevi, 15310 Athens, Greece
[6] Institute of Nuclear and Radiological Sciences, Technology, Energy and Safety, N.C.S.R. "Demokritos", Aghia Paraskevi, 15310 Athens, Greece

Abstract   *The present work concerns the preliminary analysis for the study of the (n,2n) reaction channel of the ^{165}Ho isotope at near threshold energies: 10.1, 10.4 and 10.7 MeV (E_{th}=8.04 MeV). The cross sections for the population of both the ground state ($J^\pi=1^+$) and the isomeric state ($J^\pi=6^-$, E_{ex}=139.8 keV) of the ^{164}Ho product-nucleus were measured at the afore mentioned energies via the activation technique relative to the ^{27}Al(n,α)^{24}Na and ^{197}Au(n,2n)^{196}Au reactions. The quasi-monoenergetic neutron beams were produced through the ^{2}H(d,n)^{3}He reaction in the 5.5 MV Tandem Van de Graaf accelerator of N.C.S.R "Demokritos". The preliminary experimental results are compared with theoretical predictions based on TALYS code.*

Keywords   *cross section, activation technique, isomeric state*

INTRODUCTION

The study of nuclear reactions leading to the formation of the ground and isomeric states of the product-nucleus is a sensitive tool for the validation of nuclear models. Given that the cross section ratio for the population of the ground to the population of the isomeric state is strongly dependent on the spin of these states and the spin distribution of the compound nucleus, the study of such reactions is of prime importance so as to extract information about the role of nuclear structure on the compound nucleus reactions. Towards this direction, it is important for the benchmarking of the theoretical calculations, as far as different level density models and different parametrization are concerned [1] [2].

The ^{165}Ho(n,2n) reaction populates two states of ^{164}Ho: the ground state ($J^\pi=1^+$) and the isomeric sate ($J^\pi=6^-$, E_{ex}=139.8 keV). Up to now several experimental data have been reported for both channels. However, apart from the large discrepancies, the existing data cover energies higher than 14 MeV [3]. For these reasons the validation of the theoretical calculations is hindered.

Through the present work the ^{165}Ho(n,2n)^{164}Ho^g and ^{165}Ho(n,2n)^{164}Ho^m reactions were studied for the first time at near threshold energies (E_{th}=8.04 MeV). In the following sections the experimental set-up and the data analysis methods are discussed. Moreover, preliminary results are presented along

with theoretical predictions of both channels based on different level density models of the TALYS code [4].

EXPERIMENTAL SET-UP AND METHOD

Activation Technique

The ^{165}Ho(n,2n)^{164}Ho^g and ^{165}Ho(n,2n)^{164}Ho^m reactions cross section was measured at 10.1, 10.4 and 10.7 MeV via the activation technique. This method consists of two stages: 1) The samples irradiation with quasi-monoenergetic particle beam, towards the formation of unstable product-nuclei and 2) Induced activity measurements of the product-nuclei. This method is applied when the product-nuclei have suitable decay parameters (decay mode, half-life, γ-ray energy, γ-ray intensity etc).

Accordingly, the cross section for the population of the isomeric state was calculated via Eq. 1:

$$\sigma_m = \frac{counts_m}{\Phi N_T \varepsilon_m I_m e^{-\lambda_m t_w}(1 - e^{-\lambda_m t_m})f_B} \tag{1}$$

where counts$_m$ are the counts detected for the γ-ray coming from the decay of the isomeric state, Φ is the time integrated neutron flux and N_T is the number of ^{165}Ho nuclei in the target. The quantity ε_m is the detector efficiency of the measured γ-ray at the geometry of the measurement, I_m is the intensity of the latter and λ_m is the decay constant of the isomeric state. The terms t_w and t_m stand for the "waiting time" (time interval between the end of the irradiation and the start of the measurement) and the measuring time of the activity correspondingly. The f_B factor corrects for the isomeric state decay during irradiation.

The deduction of the ground state reaction cross section is more complicated, since this state is also populated from the isomeric state (^{164}Ho$^m \to$ ^{164}Ho^g (100% IT)) [5]. Due to the half-lives of the two states, which are almost equal (28.8 min for the ground and 36.6 min for the isomeric state), the decay of the isomeric state to the ground state has to be considered during the irradiation, the waiting and the activity measurement times. Under this scope, the cross section of the ground state is given by Eq. 2:

$$\sigma_g = \frac{counts_g}{\Phi N_T \varepsilon_g I_g e^{-\lambda_g t_w}(1 - e^{-\lambda_g t_m})f_B'} -$$
$$\sigma_m \left(\frac{f_B}{f_B'} \frac{\frac{1}{\lambda_g - \lambda_m}\left(\lambda_g e^{-\lambda_m t_w}(1 - e^{-\lambda_m t_m}) - \lambda_m e^{-\lambda_g t_w}(1 - e^{-\lambda_g t_m})\right)}{e^{-\lambda_g t_w}(1 - e^{-\lambda_g t_m})} + \frac{f_c}{f_B'} \right) \tag{2}$$

The new terms appear in this equation (counts$_g$, ε_g, I_g λ_g) have the same definition as previously, but they now refer to the ground state. The terms f_B' and f_c correct for the ground state decay during irradiation.

For the neutron flux determination reference foils of Al and Au were used. Φ was calculated solving Eq. 1 to Φ, given that the cross sections of the ^{27}Al(n,α)^{24}Na and ^{197}Au(n,2n)^{196}Au reactions are well established [6].

Irradiations Set-up

Three irradiations were performed at the neutron energies of 10.1, 10.4 and 10.7 MeV. The neutron beams were produced via the ^{2}H(d,n)^{3}He reaction. In all cases the deuteron beam was provided by the 5.5 MV Tandem Van de Graaff accelerator of N.C.S.R ″Demokritos″. The deuteron

beam of intensity ~1.5 µA was directed to the D_2 gas target. The pressure of the gas target was continiously monitored and kept at 1250 mbar. The samples were irradiated at 7 cm distance from the centre of the gas cell at 0° with respect to the deuteron beam. In Fig. 1 can be seen the neutron energy distribution of the beams as resulted from NEUSDESC [7] code. In these calculations the energy loss, the angular and energy straggling of the deuteron beam across the D_2 gas target and the target structural materials were calculated through the SRIM code [8].

Three pellets were irradiated (one at each irradiation). The pellets consisted of 0.55 g of Ho_2O_3, along with a small quantity of cellulose, which enhanced the mechanical strength of the pellets. The Ho samples were ″sandwitched″ between Al and Au foils of equal diameter (13 mm). The duration of each irradiation was $\cong$ 2 h.
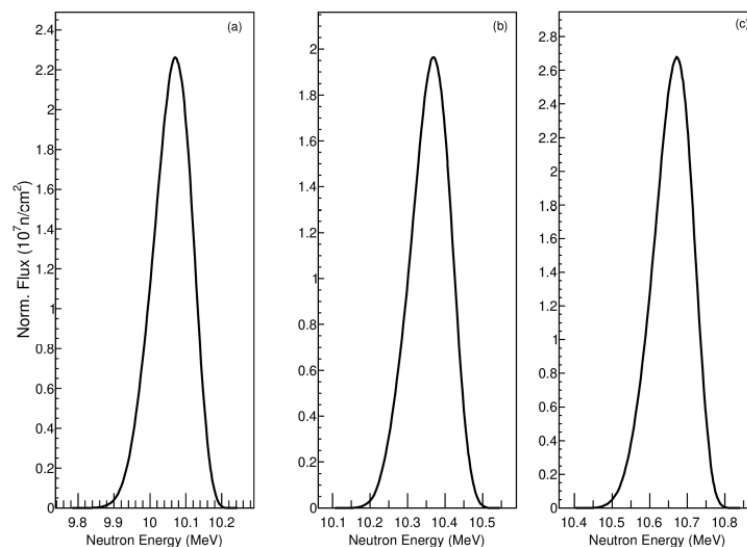
Figure 1. *Neutron energy spectra as calculated with NEUSDESC code [7] for the adopted geometry of each irradiation: (a) 10.1±0.1 MeV, (b) 10.4±0.1 MeV, (c) 10.7±0.1 MeV.*

During the irradiations the deuteron beam current fluctuations in the primary targets were recorded by means of a multichannel scaler every 10 s.

Activity measurements

After the irradiations the measurements of the induced activity of the holmium targets and the reference foils started.

For the holmium targets a broad energy HPGe detector was used (Canberra BE5030). The usage of a broad energy detector was prerequisite given that the γ-rays emitted from $^{164}Ho^{g+m}$ are located between 37.34–91.39 keV [5]. The samples were placed at 1.5 mm distance with respect to the detector window.

In order to calculate the HPGe detector full-energy peak efficiency in the geometry of the measurement for the γ-rays emitted by $^{164}Ho^{g+m}$, the detector was simulated through the GEANT4 package [9]. The simulated geometry was validated through the comparison of experimental efficiency and counting rate data (deduced using calibration sources: ^{60}Co, ^{137}Cs, ^{133}Ba, ^{241}Am, ^{210}Pb) with the corresponding results of the simulation. The results of this analysis have also been presented in the 28th HNPS Symposium Proceedings: E. Georgali et al.: **"*Characterization of the Canberra*

BE5030 Broad Energy High Purity Germanium Detector by means of the GEANT4 Monte Carlo simulation package".

The activity of the reference foils was measured in a HPGe detector with 80% relative efficiency at 1 cm distance with respect to the detector window. The full–energy peak efficiency of the detector for the geometry and the γ–rays of interest was determined through GEANT4 simulations following the previously explained procedure and using a calibration point source of ^{152}Eu in different geometries. In Fig. 2 the comparison of the experimental efficiency and counting rate data with the corresponding simulation values can be seen.
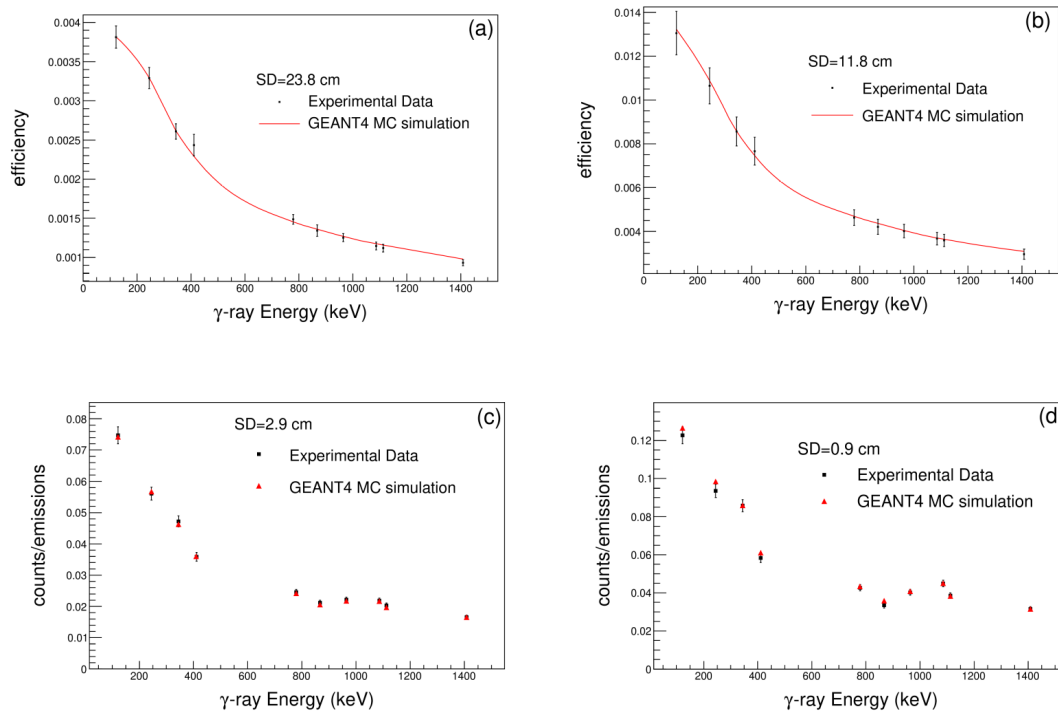
Figure 2*: Comparison of the experimental efficiency and counting rate data of the 80% relative efficiency HPGe detector with the GEANT4 MC code simulations at the distances of (a) 23.8 cm (b) 11.8 cm (c) 2.9 cm (d) 0.9 cm with respect to the detector window.*

DATA ANALYSIS

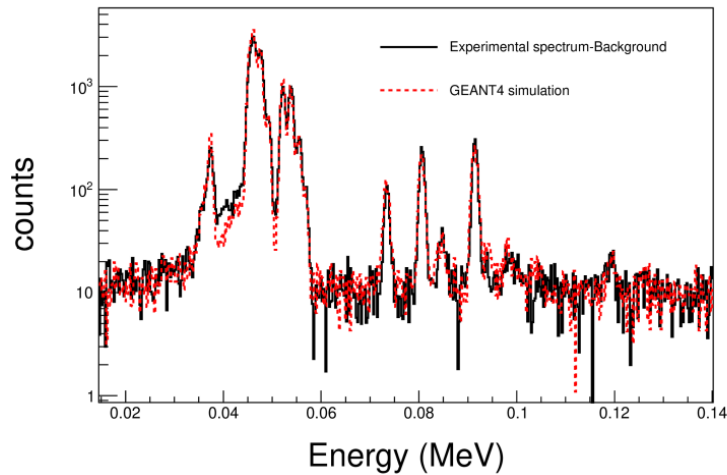### ^{165}Ho(n,2n)^{164}Ho^m reaction cross section

The cross section of the isomeric state was calculated by measuring the induced activity through the photopeak at 37.34 keV. As can be seen in Fig. 3, in which the experimental spectrum of ^{164}Ho^{g+m} decay is presented, the region of 37.34 keV is quite complicated, mainly due to the X-rays escape peaks emerging in this energy region.

Escape peaks arise when a portion of X-rays or low energy γ-rays, with energy that exceeds the energy of the Ge K-edge=11.103 keV, are absorbed by the Ge volume. In case that this energy is not recombined with the initial energy after the Ge de-excitation, it can escape from the detector active volume. As a result, escape peaks are recorded 9.87 keV (Ge K_α emission line) and 10.98 keV (Ge K_b emission line) lower in the spectrum [10]. Indeed X-rays are emitted during the ^{164}Ho^{g+m} decay with energies at 45.2, 45.99, 46.7, 47.5, 48.2 and 49.1 keV [5]. Consequently, a group of escape peaks at the 37.34 keV energy region are produced.

To take into account this phenomenon the GEANT4 code was again utilized in order to reproduce the experimental spectra after having fully characterized the BE5030 HPGe detector (see Fig. 4). In the simulations the decays of the isomeric (populated from the ^{165}Ho(n,2n)^{164}Ho^m reaction) and the ground state (populated from the ^{165}Ho(n,2n)^{164}Ho^g reaction) were handled independently. The decay of the ^{166}Ho isotope, which is produced by the ^{165}Ho(n,γ) reaction channel, was also considered. A sensitivity test was also performed trying to reproduce the experimental spectra with slightly different number of decays of the ground and the isomeric state.
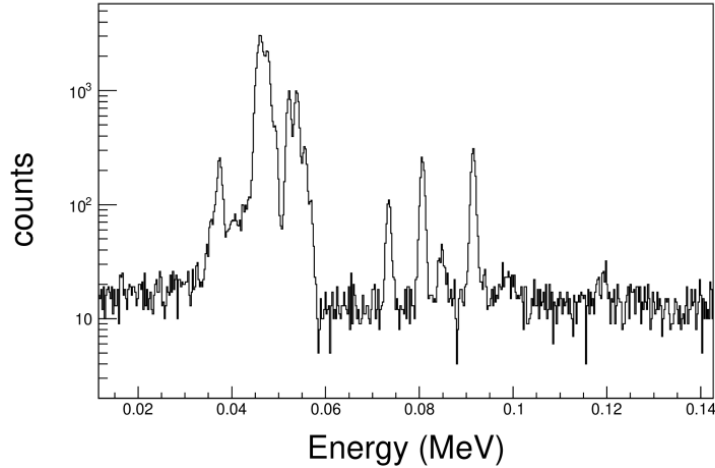
Figure 3. *The decay spectrum of ^{164}Ho^{g+m} for the neutron beam energy of 10.7 MeV and after 95 min of data acquisition time.*

Figure 4. *The experimental spectrum of ^{164}Ho^{g+m} decay for the neutron beam energy of 10.7 MeV and after 95 min of measurement against the simulation with GEANT4.*

^{165}Ho(n,2n)^{164}Ho^g reaction cross section

The determination of the ground state reaction cross section was performed using the two photopeaks at 73.39 keV and 91.39 keV. More specifically, the cross section was calculated as the weighted average of the cross sections resulting from each γ-ray and taking into consideration the existing correlation between the two values [11].

Integrated Neutron Flux

The neutron flux Φ in the holmium targets was calculated as the mean value of the flux in the front and back reference foils (Φ_1 and Φ_2 respectively):

$$\Phi = \frac{\Phi_1 + \Phi_2}{2} \qquad (3)$$

The relative uncertainty of Φ was estimated to be 7%.

RESULTS AND DISCUSSION

Through the present work the cross sections of the $^{165}Ho(n,2n)^{164}Ho^m$ and $^{165}Ho(n,2n)^{164}Ho^g$ reactions were studied at near threshold energies (E_{th}=8.04 MeV). The preliminary results of the analysis are presented in Figs. 5 and 6, for the isomeric and the ground state respectively, along with the previous data reported in the literature.

In the same figures the combination of the experimental data with theoretical calculations based on TALYS code is also presented. The performance of the latter was tested in accordance with the level density models and using the default parametrization provided by the code. The performance of the phenomenological level density models (Constant Temperature+ Fermi Gas [12], Back-Shifted Fermi Gas [13] and Generalized Superfluid [14, 15] models) is presented in Figs. 5 (left graph) and 6 (left graph) for the isomeric and ground state respectively. In Figs. 5 (right graph) and 6 (right graph) the trend of the excitation functions as resulted for the microscopic level density approach (Goriely et al. [16], Goriely et al. [17] and Hilaire et al. [18]) is presented for the isomeric and ground state respectively. As far as the preliminary data of the cross section of the isomeric state is considered, among the three phenomenological level models the Generalized Superfluid model is the one that better reproduces the present data at near threshold energies. Regarding the microscopic models none of them reproduces the preliminary data. For the cross section of the ground state, the most optimum behavior is also noticed for the Generalized Superfluid model.
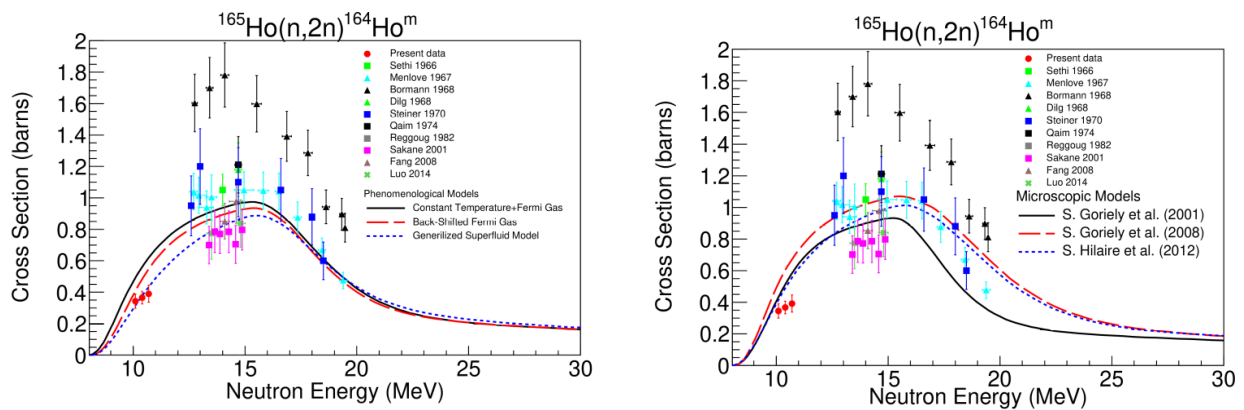
Figure 5. *The preliminary experimental data of the $^{165}Ho(n,2n)^{164}Ho^m$ reaction as resulted from the present study along with previous measurements and the theoretical predictions of the excitation function based on the phenomenological (left graph) and the microscopic (right graph) level density models of TALYS code.*
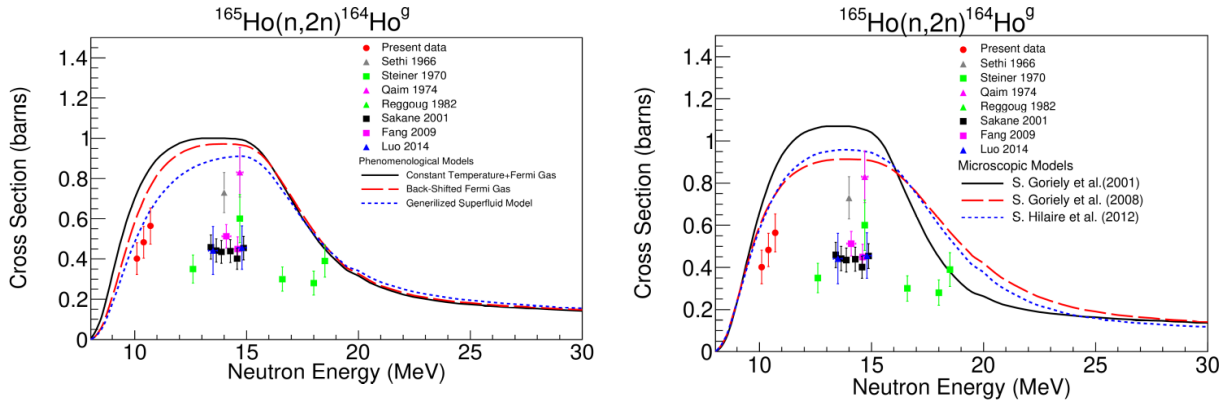
Figure 6. *The preliminary experimental data of the $^{165}Ho(n,2n)^{164}Ho^g$ reaction as resulted from the present study along with previous measurements and the theoretical predictions of the excitation function based on the phenomenological (left graph) and the microscopic (right graph) level density models of TALYS code.*
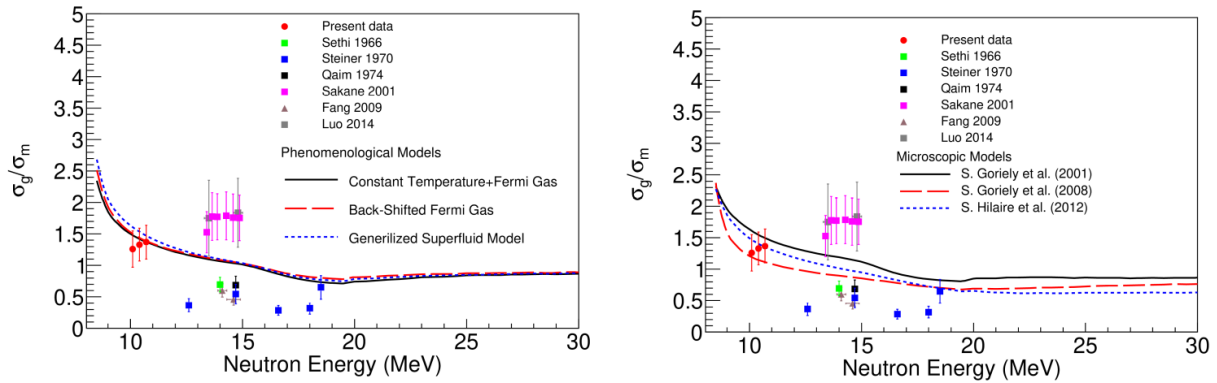
Figure 7: *The preliminary experimental ratio of the cross section of the $^{165}Ho(n,2n)^{164}Ho^g$ reaction to the cross section of the $^{165}Ho(n,2n)^{164}Ho^m$ reaction, along with previous measurements and the theoretical predictions based on the phenomenological (left graph) and the microscopic (right graph) level density models of TALYS code*
.

In Fig. 7 the ratio of the cross section of the ground state (σ_g) to the cross section of the isomeric state (σ_m) is given for the preliminary data of the present work, the previous measurements and the theoretical estimations of the phenomenological (Fig. 7 (left graph)) and microscopic (Fig. 7 (right graph)) level density models of TALYS code. Based on these figures, it is concluded that the σ_g/σ_m ratio as resulted from the present work is consistent with all the theoretical calculations (both for them correspond to the phenomenological and microscopic level density models).

CONCLUSIONS

Through the present work the cross sections of the $^{65}Ho(n,2n)^{164}Ho^m$ and $^{165}Ho(n,2n)^{164}Ho^g$ reactions were studied for the first time at near threshold energies. The results were compared with the theoretical predictions of TALYS code for different level density models. Among them the Generalized superfluid model [14,15] performed better with respect to the reproduction of the preliminary experimental results of the present work.

Acknowledgments

References

[1] N. Patronis et al., Phys. Rev. C 75, 034607 (2007).
[2] E. Georgali et al., Phys. Rev. C 98, 014622 (2018).
[3] https://www-nds.iaea.org/exfor/exfor.htm.
[4] A.J. Koning, S. Hilaire and M.C. Duijvestijn, TALYS-1.0, Proceedings of the International Conference on Nuclear Data for Science and Technology, April 22-27, 2007, Nice, France, eds. O. Bersillon, F. Gunsing, E. Bauge, R. Jacqmin, and S. Leray, EDP Sciences, 2008, p. 211-214.
[5] B. Singh and J. Chen, Nucl. Data Sheets 147, 1 (2018).
[6] International Reactor Dosimetry and Fusion File IRDFF v.1.05, 09 October, 2014; R. Capote, K.I. Zolotarev, V.G. Pronyaev, and A. Trkov, Journal of ASTM International (JAI)- Volume 9, Issue 4, April 2012, JAI104119; E.M. Zsolnay, R. Capote, H.K. Nolthenius, and A. Trkov, Technical report INDC(NDS)-0616, IAEA, 2012.
[7] E. Birgersson and G. Lovestam, JRC Science Hub Technical Report, Ref. No. 23794, (2009).
[8] J.F. Ziegler, J. P. Biersack and M. D. Ziegler, SRIM-2013. Available at http://www.srim.org.
[9] GEANT4-A simulation toolkit, S. Agostinelli et al., Nucl. Instrum. Methods. Phys. Res. A 506, 250 (2003); IEEE Transactions on Nuclear Science 53, 270 (2006); Nucl. Instrum. Methods. Phys. Res. A 835, 186 (2016)
[10] Cesar Marques Salgado, Claudio C. Conti, Paulo H. B. Becker, Applied Radiation and Isotopes 64, 700-705 (2006).
[11] N. Otuka et al., Rad. Phys. Chem. 140, 502510 (2017).
[12] A. Gilbert and A.G.W. Cameron, Can. J. Phys. 43, 1446 (1965).
[13] W. Dilg et al., Nucl. Phys. A 217, 269 (1973)
[14] A.V. Ignatyuk, K.K. Istekov, and G.N. Smirenkin, Sov. J. Nucl. Phys. 29, 450 (1979).
[15] A.V. Ignatyuk et al., Phys. Rev. C 47, 1504 (1993).
[16] S. Goriely, F. Tondeur, and J.M. Pearson, At. Data Nucl. Data Tables 77, 311 (2001).
[17] S. Goriely, S. Hilaire, and A.J. Koning, Phys. Rev. C 78, 064307 (2008).
[18] S. Hilaire et al., Phys. Rev. C 86, 064317 (2012).